Robotica (2024), **42**, pp. 3639–3656
doi:10.1017/S0263574724001565

CAMBRIDGE UNIVERSITY PRESS

RESEARCH ARTICLE

Optimisation of synchronisation control parameters for enhanced bilateral teleoperation system

Naveen Kumar, Niharika Thakur and Yogita Gupta

Department of Electronics and Communication Engineering, Manav Rachna University, Faridabad, Haryana, India
Corresponding author: Niharika Thakur; Email: niharika0023@gmail.com

Received: 4 April 2024; **Revised:** 30 July 2024; **Accepted:** 21 August 2024; **First published online:** 8 October 2024

Keywords: bilateral teleoperation systems; sequential quadratic programming (SQP); PID controllers; synchronisation errors

Abstract

Bilateral teleoperation systems encounter challenges in achieving synchronisation between master and slave robots due to communication time delays. This paper addresses the instability caused by these delays and proposes a solution through advanced control algorithms. Nonlinear optimisation algorithms might only sometimes deliver solutions in the allotted time, particularly when handling complicated, high-dimensional issues or when optimisation iterations are extensive. The study first develops a comprehensive mathematical model encompassing the dynamics and communication intricacies of both master and slave sides in teleoperation. By recognising the limitations of existing proportional-derivative controllers in compensating for communication errors, a sequential quadratic programming-proportional-integral-derivative (SQP-PID) controller is introduced. This controller accumulates and rectifies synchronisation delay errors, ensuring precise control without steady-state deviations. The proposed SQP-PID controller stands out for its ability to handle steady-state errors effectively, offering swift response and maintaining stability. Leveraging the SQP optimisation algorithm, it intelligently tunes the parameters, minimising synchronisation errors. The approach capitalises on the simplicity, performance, and robustness of the SQP-PID controller, providing a promising avenue for enhancing bilateral teleoperation systems' accuracy and stability, maintaining initial discrepancy with a best fitness value of 0.98 % in varied operating conditions.

1. Introduction

Teleoperation systems [1] have become essential in modern technology and distant operations, especially when there is a risk, the location is remote, or the distance is excellent [2]. These developments increase chances for exploration and intervention while reducing threats to human safety by enabling people to operate machinery and equipment from a distance [3]. However, achieving smooth and efficient synchronisation between the operator's inputs and the remote system's responses is crucial to teleoperation's success [4]. The utilisation of optimisation techniques to improve synchronisation has been spurred by this challenging problem, which has improved teleoperation systems' efficacy and efficiency. These systems are used in many industries, including industrial manufacturing, deep-sea research, space missions, and medicine [5]. Succeeding in these settings requires exact synchronisation between the operator's activities and the distant system's behaviour [6]. Synchronisation precision may be compromised by external variables, system dynamics, and communication latency [7]. These complications may only partially be resolved by traditional control methods.

Optimisation techniques provide a robust framework for managing complex synchronisation issues in teleoperation systems [8, 9]. Through an optimisation-based approach [10] to the synchronisation problem, researchers and engineers can optimise control algorithms, communication protocols, and system characteristics to reach optimal performance. These strategies not only deal with communication lags but also adjust to unforeseen environmental changes and real-time changes in system dynamics. Various optimisation strategies, including convex optimisation, evolutionary algorithms, reinforcement learning

© The Author(s), 2024. Published by Cambridge University Press.

https://doi.org/10.1017/S0263574724001565 Published online by Cambridge University Press

(RL), and model predictive control (MPC), are frequently necessary to achieve optimal synchronisation [11]. To effectively compensate for system uncertainties and communication delays, MPC, for example, enables teleoperation systems to predict future states and optimise control inputs. Natural selection principles are utilised by evolutionary algorithms to gradually improve control strategies over time, adapting them to changing conditions and increasing synchronisation precision [12].

Furthermore, the application of artificial intelligence and machine learning (ML) improves the efficiency of optimisation methods for coordinating teleoperation [13]. RL interacts with the environment to help systems understand the optimal synchronisation techniques, resulting in flexible and context-aware management. Furthermore, convex optimisation techniques offer effective means of quickly modifying control parameters, guaranteeing optimal synchronisation even in dynamic and unpredictably changing operating circumstances [14]. Achieving flawless coordination between operators and distant systems is essential in remote operations. Algorithms for optimisation provide a potent remedy for this. Researchers and engineers can improve the accuracy, flexibility, and overall performance of synchronisation in systems by applying MPC, evolutionary algorithms, RL, and convex optimisation. As technology develops and the demand for dependable teleoperation increases, incorporating these optimisation techniques into teleoperation systems is set to transform remote operations across various industries and applications. The contribution of this research is as follows:

- A novel framework, sequential quadratic programming-proportional-integral-derivative (SQP-PID), is proposed, which addresses the dynamics and communication intricacies of both master and slave sides in teleoperation.
- The synchronisation delay issues are corrected through the design of the SQP-PID controller, which ensures accurate control with no steady-state deviations.
- It maintains system stability while providing a quick response to minimise synchronisation errors by carefully adjusting the PID parameters using the SQP optimisation technique.
- It significantly decreased synchronisation errors by fine-tuning the controller's parameters.

The structure of this section of the study is as follows: Section 2 describes the literature review, Section 3 describes the recommended approach, Section 4 provides results and analysis with findings, and Section 5 provides a conclusion.

2. Literature survey

Honghao Lv et al. [15] presented GuLiM, a method for synchronising motion that merges upper-limb movement with hand gestures. This technique streamlines operations and reduces the need for extensive training among healthcare workers. Experimental results indicate that GuLiM outperforms traditional direct mapping methods and holds promise for remotely controlling medical assistance robots in isolated wards to minimise COVID-19 exposure. Additionally, a field investigation is conducted to validate the effectiveness of this methodology.

Yunpeng Su et al. [16] emphasise reducing latency in telemanipulation tasks, primarily when overseeing intricate robotic systems. Constraints in hardware often lead to performance gaps due to significant delays in teleoperation. To address this, ML methods like hidden Markov models (HMMs) can bridge these limitations. They propose a teleoperation system enhanced with mixed reality incorporating an HMM generative algorithm to anticipate human-welder movements. This cost-effective solution significantly decreases teleoperation delays, exhibiting a 66% reduction in root mean square error compared to a system without HMM. The outcomes of the experiments show that the HMM generative algorithm notably enhances the performance of human-robot-assisted welding.

Hamid Shokri-Ghaleh et al. [17] developed Unequal Limit COA (ULCOA), a modified version of the Cuckoo Optimisation Algorithm (COA), to obtain the optimal calibration parameters. By putting ULCOA through various nonlinear benchmark functions, they evaluated its efficacy and found that it

https://doi.org/10.1017/S0263574724001565 Published online by Cambridge University Press

performed more accurately and robustly than genetic algorithms (GA) and particle swarm optimisation (PSO). They also discussed ULCOA in-field calibration and its use in calibrating the triaxial MEMS accelerometer. In the end, they performed.

Waheed Ur Rehman et al. [18], a servo-hydraulic actuator and an electromechanical actuator, are the two actuators for which the study suggests a nested-loop control technique. The feed-forward controller, intelligent force controller, trajectory controller, and smart position controller are all part of this method. Matlab/Simulink simulations demonstrate improved output-trajectory tracking, load rejection, and decreased force inconsistencies.

Leila Mohammadi et al. [19] introduced a control framework to attain stability without delay dependence in bilateral teleoperation setups when dealing with actuator saturation. Their research applies the Razumikhin theorem to analyse stability, handling issues arising from time delay and nonlinearities caused by control input saturation. They devised a control structure based on transparency and integrated a guaranteed cost controller to ensure both stability and transparency. To determine the best parameters, they utilised convex optimisation. Simulations demonstrated the control structure's compelling performance.

Yasuhiro Ishiguro et al. [20] outlined a method for designing a system to enable two-way remote control of a humanoid robot. They focused on ensuring stability while walking on two legs and addressing the complexities of moving in 2D and 3D spaces. The system included the revolutionary "TABLIS" full-body exoskeleton cockpit and master software, which simulates a far-off ground surface to enable navigation despite space restrictions. Additionally, the software on the robot's side prevents potential collapses caused by inaccurate inputs.

Fawad Naseer et al. [21] introduced a combined method to aid a telepresence robot in navigating delayed operating signals. This technique combines deep RL with a duelling double-deep Q-network (DDQN). The DDQN determines the optimal control strategy, while gated recurrent unit models handle temporal dependencies in control signals. This approach significantly boosts tracking precision and stability, enabling the robot to autonomously handle activities even with 15-s delays, marking a 2.4% advancement compared to existing methods. The effectiveness of this hybrid approach demonstrates how RL and deep learning may be used to improve telepresence robot control and stability.

3. Research methodology

In bilateral teleoperation control setups, a delay happens when signals transfer between the owner and the employee robots. Designing controllers for these systems means balancing between transparency and stable performance. When the master and slave positions match, the teleoperation achieves full transparency, presenting the human operator with precisely the environmental reaction force. Yet, because there's no feedback signal from the slave to the master, the operator at the master end can't naturally sense the interaction between the environment and the slave manipulator. Consequently, controlling the slave object accurately, especially considering interaction forces, becomes challenging. As the need for precise and safe remote operations grows, there's a push for teleoperation systems that can sense the environment, promoting the creation of systems for bilateral teleoperation.

In this research, the mathematical model for the bilateral teleoperation system has been formulated, encompassing the dynamics of both the master and slave components, factoring in delays and communication network effects. A significant focus in control research involving time delay systems pertains to teleoperation systems. In an existing paper, a proportional-derivative controller is implemented to tackle communication errors that lack integral action. Figure 1 shows the proposed architecture for the bilateral teleoperation systems.

This research examines the impact of communication delays on the precise movement of a robotic arm, revealing instability in the system. Numerous control algorithms have been suggested to counter this issue, yet they often need to catch up when dealing with the complex dynamics of nonlinear robotic systems. Traditional tuning methods lack the adaptability required for such nonlinear systems, hindering

https://doi.org/10.1017/S0263574724001565 Published online by Cambridge University Press

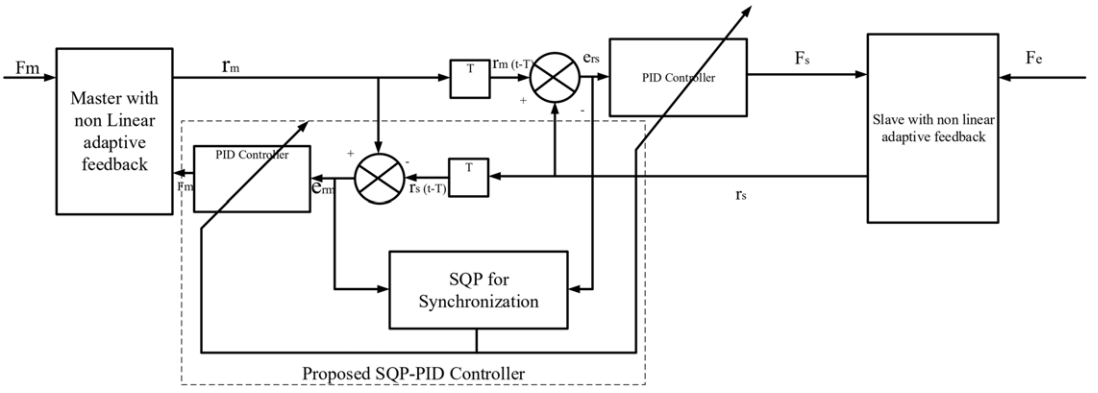


Figure 1. *Proposed model.*

performance, stability, and error correction. Thus, there's a pressing need for more effective approaches to determine controller parameters for these nonlinear systems. One potential method involves treating these systems as multi-input and multi-output systems and applying standard tuning rules or gain scheduling across various operational points. However, optimising algorithms becomes crucial to search for the best gain parameters, ultimately enhancing system performance.

Thus, this research proposed an SQP-PID controller that addresses the above limitation by accumulating and rectifying synchronisation delay errors over time, effectively preventing steady-state errors. This method leverages a PID controller, offering swift responses and precise steady-state control to avoid synchronisation discrepancies between the master and slave components. This controller effectively manages constant errors, ensuring precise control and swift adjustment, allowing the variable to settle rapidly while maintaining stability. The sequential quadratic programming (SQP) optimisation algorithm utilises quasi-Newton's method to optimise tuning parameters, enhancing the synchronisation. This method immediately addresses the KKT condition of the original problem. The nonlinear teleoperator's dynamical model and the presumptions required for the controller's stability analysis are presented in the following section.

3.1. Modelling of bilateral teleoperators

Given the absence of friction and other disruptive factors, the Euler–Lagrange equations describe the motion of n-connection robots for the master and slave can be presented as

$$M_m(q_m)\dot{q}_m + C_m\left(q_m, \dot{q}_m\right)\dot{q}_m + g_m(q_m) = F_h + \tau_m \tag{1}$$

$$M_s(q_s)\dot{q}_s + C_s\left(q_s, \dot{q}_s\right)\dot{q}_s + g_s(q_s) = \tau_s - F_e \tag{2}$$

where $q_m, q_s \in \mathbb{R}^n$ are the joint displacement vectors, $\tau_m, \tau_s \in \mathbb{R}^n$ are the control input torques, and $F_h, F_e \in \mathbb{R}^n$ are, in turn, the force exerted by the environment and the force used by the human operator. $M_m, M_s \in \mathbb{R}^{n\times n}$ are the inertia matrices, $C_m\dot{q}_m, C_s\dot{q}_s \in \mathbb{R}^n$ are the vectors of centrifugal and Coriolis torque, and $g_m, g_s \in \mathbb{R}^n$ are the gravitational torque vectors. The subscripts s and m represent the slave and master robots from {1, 2,. . ..., N}, based on the number of slaves connected with the master.

The inertia matrix $M(q)$ is limited, symmetric, and positive definite as follows:

$$\lambda_m I_{n\times n} \le M(q) \le \lambda_M I_{n\times n} \tag{3}$$

where λ_m, λ_M are the eigenvalues of the lowest and maximum $M(q)$ correspondingly and $I_{n\times n} \in \mathbb{R}^{n\times n}$ is the identity matrix.

Using the matrix of inertia $M(q)$ as well as the matrix Coriolis/centrifugal and the$C(q, \dot{q})$, the matrix $\dot{M}(q) - 2C(q, \dot{q})$ has a skew symmetry.

https://doi.org/10.1017/S0263574724001565 Published online by Cambridge University Press

The n-link robot's equations of motion can be linearly parameterised as

$$M(q)\ddot{q} + C(q, \dot{q})\dot{q} + g(q) = Y(q, \dot{q}, \ddot{q})\Theta \tag{4}$$

where $Y(q, \dot{q}, \ddot{q}) \in \mathbb{R}^{n\times l}$ is a known function matrix, referred to as a regressor, and $\Theta \in \mathbb{R}^{l}$ is a vector with unidentified dimensions.

The following models assume that the human operator and external factors are non-passive:

$$F_h\,(t) = -K_{h0} + K_{hq_m} + C_h\dot{q}_m \tag{5}$$

$$F_{si}\,(t) = -K_{e0} + K_{eq_i} + C_e\dot{q}_i \tag{6}$$

where $K_{w0}, K_w, C_w \in \mathbb{R}^{n\times n}, w = \{h, e\}$.

Let us define d_{mi}(t) as the slave's master's tardiness*i* and d_{mi}(t) as the slave's delay i to the master.

3.1.1. Control objectives

A system transformation is first performed to control the coupled nonlinear dynamics of the closed-loop system. The following synchronisation signals should be defined:

$$r_m\,(t) = \dot{q}_m\,(t) + A_m q_m(t) \tag{7}$$

$$r_i\,(t) = \dot{q}_i\,(t) + A_i q_i(t) \tag{8}$$

Stability and transparency are the primary concerns of bilateral teleportation systems. Our goal is to create control inputs, e_m, e_x, to ensure system stability and accomplish transparency in a coordinated manner.

where Λ_{m} and $\Lambda_i, i = \{1, 2, \cdots, N\}$ are diagonal matrices that are positive definite.

Additionally, define

$$\dot{q}_{mr}(t) = -\Lambda_m q_m(t), \dot{q}_{ir}(t) = -\Lambda_i q_i(t), \tag{9}$$

$$\mu_m(t) = M_m\,(q_m)\,\overleftarrow{y}_{\mathrm{mor}}(t) + C_m\left(q_m, \dot{q}_m\right)\dot{q}_m(t) + G_m\,(q_m)\,q_m(t) - F_h(t) \tag{10}$$

$$\mu_i(t) = M_i\,(q_i)\,\dot{q}_{ir}(t) + C_i\left(q_i, \dot{\phi}_i\right)\dot{q}_i(t) + G_i\,(q_i)\,q_i(t) - F_{si}(t) \tag{11}$$

Using (9)–(11), (1) can be rewritten as

$$M_{\mathrm{m}}\,(q_{\mathrm{m}})\,\dot{r}_{\mathrm{m}}(t) = \tau_{\mathrm{m}}(t) - \mu_{\mathrm{m}}(t) \tag{12}$$

$$M_i\,(q_{\mathrm{i}})\,\dot{r}_{\mathrm{i}}(t) = \tau_i(t) - \mu_i(t). \tag{13}$$

Now employ the nonlinear feedback control theory by defining the control signals as follows:

$$\tau_m(t) = M_m\,(q_m)\left(u_m(t) + M_m^{-1}\,(q_m)\,\mu_m(t)\right) \tag{14}$$

$$\tau_i(t) = M_i\,(q_i)\left(u_i(t) + M_i^{-1}\,(q_i)\,\mu_i(t)\right) \tag{15}$$

where$u_m(.)$ and $u_1($ are auxiliary control variables, with which the dynamics of coordination errors can be formulated as follows:

$$\dot{e}_{\mathrm{m}}\,(t) = \frac{\mathrm{d}}{\mathrm{d}t}\left[k_{\mathrm{m}}q_{\mathrm{m}}\,(t) - k_{\mathrm{mj}}\frac{1}{N}\sum_{i=1}^{N}\,q_i\,(t - d_{\mathrm{mm}}\,(t))\right] \tag{16}$$

$$\begin{aligned} =& -\Lambda_{\mathrm{m}}\varepsilon_m\,(t) - \frac{k_{\mathrm{m}}}{N}\sum_{i=1}^{N}\,(\Lambda_m - \Lambda_i)\,q_i\,(t - d_{im}\,(t)) - \frac{k_{\mathrm{m}}I}{N}\sum_{i=1}^{N}\,(1 - d_{im}\,(t)) \times r_i\,(t - d_{im}(t)) \\ &+ k_m r_m(t) - \frac{k_m I}{N}\sum_{i=1}^{N}\,d_{im}(t)\Lambda_i q_i\,(t - d_{im}(t)) \end{aligned} \tag{17}$$

https://doi.org/10.1017/S0263574724001565 Published online by Cambridge University Press

$$\dot{e}_i(t) = \frac{\mathrm{d}}{\mathrm{d}t}\left[k_i q_i(t) - k_{im} q_m\left(t - d_{ma}(t)\right)\right] \tag{18}$$

$$\begin{aligned} &= -\Lambda_i e_i(t) - k_{im}\left(\Lambda_i - \Lambda_m\right) q_m\left(t - d_{mi}(t)\right) - k_{im}\Lambda_m \grave{d}_{mi} q_m\left(t - d_{mi}\right) \\ &\quad + k_i r_i(t) - k_{im}\left(1 - \grave{d}_{mi}(t)\right) r_m\left(t - d_{mi}(t)\right) \end{aligned} \tag{19}$$

Define

$$e\left(t\right) = \left[e_m^T\left(t\right), \mathbf{e}_s^T\left(t\right)\right]^T \tag{20}$$

$$\mathbf{e}_s(t) = \left[e_1^T(t), \cdots e_N^T(t)\right]^T, \boldsymbol{r}(t) = \left[\boldsymbol{r}_m^T(t), \mathbf{r}_s^T(t)\right]^T, \boldsymbol{r}_m(t) \tag{21}$$

$$= \left[r_m^T(t), \cdots, r_m^T(t)\right]^T, \boldsymbol{r}_s(t) = \left[r_1^T(t), \cdots, r_N^T(t)\right]^T \tag{22}$$

$$X(t) = \left[e^T(t), \boldsymbol{r}^T(t)\right]^T. \tag{23}$$

Consequently, it is possible to deduce the robot's dynamics from the augmentation of the error and synchronisation signals.

Considering Synchronisation error, which is the time lag in the communication channel between the slave and master robots, may be expressed as

$$e_m(t) = q_x(t - T) - q_m(t) \tag{24}$$

$$e_i(t) = q_m(t - T) - q_x(t) \tag{25}$$

Consequently, bilateral teleoperators' synchronisation might be described as

$$\lim_{t\to\infty} e_m(t) = \lim_{t\to\infty} e_i(t) = 0 \tag{26}$$

Achieving force reflection from the remote environment in a contact situation is also crucial.

$$F_h = F_{\mathrm{c}} \text{ with } \grave{q}_m(t) = \leftarrow q_x(t) = \grave{q}_m(t) = \grave{q}_s(t) = 0.$$

An adaptive technique is used to estimate parameters while taking modelling uncertainty into account. A nonlinear adaptive feedback controller is built using the new output variables, a linear combination of position and velocity. Create the nonlinear adaptive feedback compensation's control input torques as

$$\tau_m = -\grave{M}_m\left(q_m\right)\lambda\grave{q}_m - \grave{C}_m\left(q_m, \grave{q}_m\right)\lambda q_m + \grave{g}_m\left(q_m\right) + F_m \tag{27}$$

$$\tau_x = -\grave{M}_x\left(q_s\right)\lambda\grave{q}_x - C_x\left(q_s, \grave{q}_s\right)\lambda q_x + \grave{g}_x\left(q_x\right) + F_x \tag{28}$$

where $\hat{M}_{\mathrm{m}}, \hat{M}_x, \hat{C}_m, \hat{C}_x, \hat{g}_m, \hat{g}_x$ are estimated parameters as a result of robot manipulators' modelling uncertainty, $\lambda \in \mathbb{R}^{\mathrm{n}\times\mathrm{n}}$ is a matrix with positive definiteness, and F_{m}, F_n are extra control inputs that help with synchronisation.

$$\begin{aligned} M_m\left(q_m\right)\left(\leftarrow q_m + \lambda\grave{q}_m\right) + C_m\left(q_m, \grave{q}_m\right)\left(\grave{q}_m + \lambda q_m\right) &= F_h + \overleftarrow{M}_m\left(q_m\right)\lambda\grave{q}_m + \overleftarrow{C}_m\left(q_m, \grave{q}_m\right)\lambda q_m \\ &\quad - \overleftarrow{g}_m\left(q_m\right) + F_m \end{aligned} \tag{29}$$

$$\begin{aligned} M_x\left(q_x\right)\left(\overleftarrow{q}_x + \lambda\grave{q}_x\right) + C_x\left(q_x, \grave{q}_x\right)\left(\grave{q}_x + \lambda q_x\right) &= -F_c + \overleftarrow{M}_x\left(q_x\right)\lambda\grave{q}_n + \overleftarrow{C}_x\left(q_x, \grave{q}_x\right)\lambda q_n \\ &\quad - \overleftarrow{g}_x\left(q_s\right) + F_x \end{aligned} \tag{30}$$

where $\grave{M}_i = M_i - \grave{M}_i, \grave{C}_i = C_i - \grave{C}_i, \grave{g}_i = g_i - \grave{g}_i (i = m, s)$ are parameter estimation errors.

$$M_m\left(q_m\right)\grave{r}_m + C_m\left(q_m, \grave{q}_m\right) r_m = F_h + F_m + Y_m\left(q_m, \grave{q}_m\right)\grave{\Theta}_m \tag{31}$$

https://doi.org/10.1017/S0263574724001565 Published online by Cambridge University Press

$$M_s(q_s)\dot{r}_s + C_s\left(q_s, \dot{q}_s\right) r_s = -F_e + F_s + Y_s\left(q_s, \dot{q}_s\right)\dot{\Theta}_s \tag{32}$$

where $Y_m(q_m, \dot{q}_m)$, $Y_s(q_s, \dot{q}_s) \in \mathbb{R}^{n\times l}$ are regressor matrices, $\dot{\Theta}_m$, $\dot{\Theta}_s \in \mathbb{R}^l$ are parameter estimation error vectors, and r_m, r_s are new output variables defined as

$$r_m = \dot{q}_m + \lambda q_m \tag{33}$$

$$r_s = \dot{q}_s + \lambda q_s \tag{34}$$

To estimate unknown parameters, parameter update laws are selected as

$$\dot{\hat{\theta}}_m = \Gamma Y_m^T r_m \tag{35}$$

$$\dot{\hat{\theta}}_s = \Lambda Y_s^T r_s \tag{36}$$

where Γ, $\Lambda \in \mathbb{R}^{n\times n}$ are positive definite matrices.

PID controllers are used as additional control inputs for synchronisation control. The master and slave synchronisation is the focus of this control input. The term "synchronisation error" may be redefined by using additional output variables as

$$e_{Tm}(t) = r_s(t-T) - r_m(t) \tag{37}$$

$$e_{rs}(t) = r_m(t-T) - r_s(t) \tag{38}$$

To get synchronisation, we create extra control inputs. F_m, F_s as

$$F_m = Kpe_{Tm}(t) + K_D\dot{e}_{rm}(t) \tag{39}$$

$$F_s = K_p e_{Ts}(t) + K_D\dot{e}_{rs}(t) \tag{40}$$

where K_p, $K_D \in \mathbb{R}^{n\times n}$ are diagonal matrices that are positive definite. To keep things simple, it is assumed that $Kp = k_p I_{n\times n}$, $K_D = k_d I_{n\times n}$ where $k_p, k_d \in \mathbb{R}$, $I_{n\times n} \in \mathbb{R}^{n\times n}$ is the identity matrix. These control gain matrices can be optimised by a PID controller based on SQP, which optimises control parameters in a bilateral teleoperation system to minimise time delay and synchronisation error. This entails setting the PID controller's initial parameters and modifying them repeatedly by figuring out sub-problems in quadratic programming that almost correspond to the nonlinear optimisation task. The time delay and synchronisation error are measured at each iteration, providing the foundation for minimising the objective function. SQP provides accurate management of nonlinear goals and constraints, which results in optimal performance and convergence to control satisfactory parameter values. The flexibility of PID control and the optimisation power of SQP provide improved teleoperation systems, convergence qualities, and performance.

3.2. PID parameters tuning using SQP

A simple control structure is the feedback control structure, in which the automatic controller compares the actual value of the plant output to the reference input (desired value), calculates the deviation, and generates a control signal to reduce the deviation to zero or a small value.

One possible component of the control in the above structure is a PID controller, which is based on three fundamental behaviour types: derivative (D), integral (I), and proportional (P). The proportional action produces a control signal proportionate to the error between the reference signal and the actual output. While the derivative action offers a derivative signal of the mistake, the integral action provides an essential signal of the error. The relation between the control $n(t)$ and error $e(t)$ can be expressed in the following form:

$$u(t) = K_p\left[\epsilon(t) + \frac{1}{T_i}\int_0^t \epsilon(\tau)d\tau + T_d\frac{d}{dt}\epsilon(t)\right] \tag{41}$$

https://doi.org/10.1017/S0263574724001565 Published online by Cambridge University Press

Kp, Ti, and Td are the parameters to be tuned. The corresponding transfer function is given by

$$K(s) = K_f \left(1 + \frac{1}{T_i s} + T_d s\right) \tag{42}$$

The Matlab Toolbox's Nonlinear Control Design (NCD) block set is a tool for adjusting PID controller settings and identifying process attributes. It is employed to establish controller settings and retrieve process variables. The NCD block set transforms constraints and simulated system output into an optimisation problem to satisfy time domain performance requirements in a nonlinear Simulink model. In process control, this guarantees that the PID controller's time will continue to be significant.

$$min_{x,y}\ \gamma\ s.t.\ \begin{cases} g(x) - w\gamma \leq 0 \\ x_l \leq x \leq x_w \end{cases} \tag{43}$$

This work presents an approach that uses the SQP optimisation technique to minimise the maximum constraint error in an NCD block set. The variable x represents tumble variables, and tumble variables' lower and upper limits are defined by the variables xl andxu. Vectorisation is used for the constraint bound and constraint weighting. After resolving the Karush–Kuhn–Tucker (KKT) condition, the SQP algorithm minimises a quadratic approximation of the Lagrangian function over a linear approximation of constraints, which becomes a sub-problem. The suggested SQP-PID controller holds great potential for bilateral teleoperation systems due to its simplicity, strong performance, accurateness, and the availability of efficient yet straightforward tuning methods to minimise synchronisation errors.

4. Result and discussion

4.1. Sequential quadratic programming with KP

In the realm of optimisation algorithms, the SQP method is a powerful tool that seeks to enhance the performance of a given function iteratively. In this particular scenario, the fitness function graph for SQP is intricately tied to a proportional constant, denoted as Kp. As the algorithm embarks on its journey of iterations, the fitness landscape unfolds dynamically. At the outset, the fitness value stands tall at 14 e4, representing an initial state of the system. However, the optimisation process unfolds its prowess, initiating a sudden descent in fitness, a testament to the algorithm's ability to refine the solution rapidly. Figure 2 illustrates a significant drop to a fitness level of 5 e4, signifying a notable improvement in the system's performance. Subsequently, the fitness curve gradually descends, steadily progressing towards greater efficiency. Notably, by the 30th iteration, the fitness function gracefully reaches a low of 2 e4, underscoring the SQP algorithm's persistent fine-tuning and optimisation capabilities. This graph visualises the iterative journey towards an increasingly optimal solution, guided by the influential constant Kp. SQP facilitates accurate adjustment of the proportional constant (KP) to attain the intended system response. KP tuning is essential to ensure the system reacts to faults effectively and doesn't overrun or cause excessive oscillations. It makes sure that the control system stays stable by optimising KP. This helps to avoid problems like instability or long-lasting oscillations that might occur from improperly adjusted proportional gains.

4.2. Sequential quadratic programming with K_d

The fitness function graph is a visual optimisation narrative in SQP accompanied by a derivative constant (Kd). At the onset, the fitness score loomed at a staggering 2.03e5, portraying a landscape of inefficiencies and deviations. However, the algorithm's strategic manoeuvres swiftly induced a marked descent, plunging to 2.01e5 within a concise timeframe, indicating an abrupt rectification in the system. This rapid shift was akin to an orchestrated symphony of adjustments, steering towards enhanced efficiency. As the iterations progressed, a deliberate and gradual descent ensued, illustrating a consistent refinement in performance. By the 30th iteration, the fitness function graph exhibited a commendable stature,

https://doi.org/10.1017/S0263574724001565 Published online by Cambridge University Press

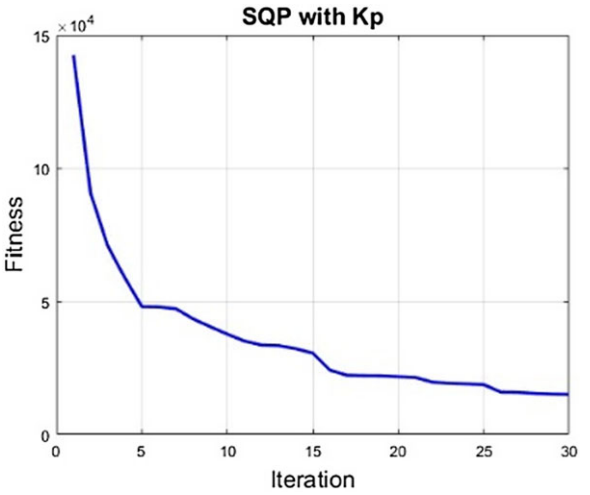


Figure 2. *SQP with K_p.*

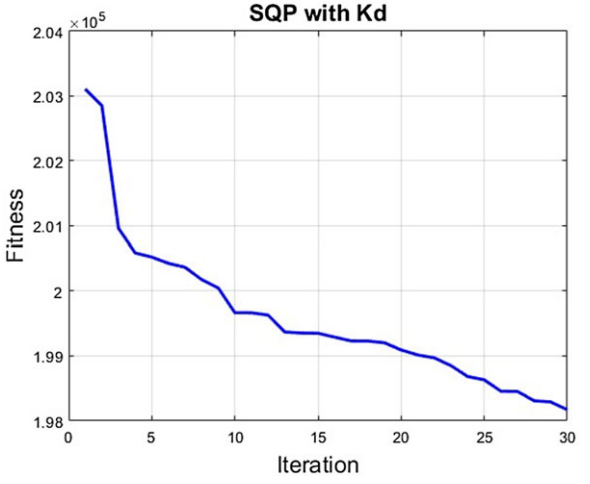


Figure 3. *SQP with Kd.*

boasting a refined fitness score of 1.98e5. In Fig. 3, this gradual yet persistent decline epitomised the algorithm's calibrated precision and adaptability, illustrating its prowess in converging towards optimal solutions methodically. The derivative constant is carefully adjusted using SQP to enhance the system's response to changes. The derivative component reduces oscillations and improves stability by using the current rate of change to predict future errors. The optimal damping effect can be achieved by optimising the Kd value using SQP while avoiding instability or undue control effort.

4.3. Sequential quadratic programming with K_{PID}

In the landscape of SQP with proportional-integral-derivative (PID) control, the fitness function graph is a visual symphony of optimisation. At the outset, the fitness function soared to a formidable 16e4, an imposing peak challenging the algorithm. As the iterations commenced, the PID control strategised and manoeuvred, orchestrating a swift and surprising descent in fitness, a plunge akin to a free fall, steadily carving through obstacles, arriving at 5e4 – a notable accomplishment in a short span. However, the journey was far from over. What followed was a nuanced narrative of perseverance; the graph portrayed

https://doi.org/10.1017/S0263574724001565 Published online by Cambridge University Press

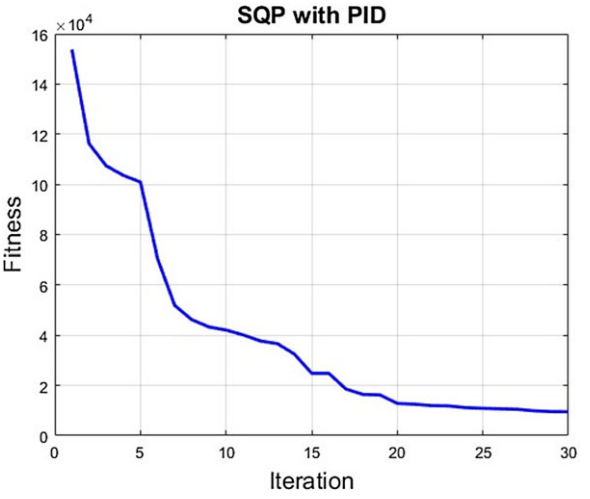


Figure 4. *SQP with PID.*

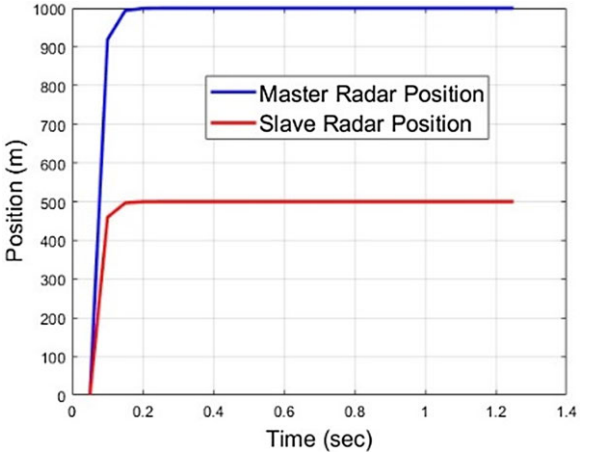


Figure 5. *Master and slave radar position.*

a gradual decline in fitness, akin to a meticulously planned descent down a winding mountain trail. At the 30th iteration, the fitness stood at a commendable 1e4, a testament to the precision and adaptability of the SQP with PID, showcasing its capacity to navigate complexities and optimise towards the desired outcome. SQP optimises the KPID controller's proportional, integral, and derivative gains to maximise response time, stability, and error reduction. SQP successfully controls the dynamics of the system's nonlinearities, guaranteeing that the KPID controller operates well across various operational environments and disruptions. Figure 4 encapsulates the dynamic tale of optimisation, showcasing the methodical evolution from challenge to triumph through iteration and precision engineering.

4.4. Radar positioning

In radar positioning, the dynamics between master and slave positions unfold fascinatingly. Figure 5 shows that at a mere 0.1 s into the sequence, the master and slave signals surge forth with a steep rise on the graph, a testament to their synchronised initiation. A sudden increase in the master signal indicates the start of the radar activity. The master radar system begins transmitting signals or positional data

https://doi.org/10.1017/S0263574724001565 Published online by Cambridge University Press

Table I. *Time domain versus position domain.*

Gain level	Time domain ($10^{-3}s$)	Position domain ($10^{-3}m$) [22]
Low gain (Kp)	0.109	14.8
Middle gain (K_d)	0.293	3.1
High gain (K_{PID})	0.054	1.5

immediately, as shown by the sudden and abrupt spike on the graph. Mirroring the master's first surge, the slave signal also indicates a high ascend simultaneously. It is essential to have this synchronised initiation to guarantee that the slave and master systems are operating simultaneously from the beginning. The master, a stalwart beacon, maintains its unwavering presence at a resolute altitude of 1000m.

Meanwhile, the slave, harmonising in the symphony of radar echoes, mirrors this ascent with an equally steep climb, settling distinctly but confidently at a steady 500 m. This visual representation encapsulates the interplay of supremacy and synchronisation, where the master leads the charge. At the same time, the slave follows suit, each asserting their defined position with an eloquent precision that mirrors the artistry of radar technology. Table I represents the comparison of gain level on time and position domain.

Table I presents a performance comparison of the three different gain levels (low gain (Kp), middle gain (K_d), and high gain (K_{PID}) in the time and position domains in the context of control systems. To be more precise, the steady-state error in millimetres ($10^{-3}m$) represents the position domain, and the time constant in milliseconds ($10^{-3}s$) represents the time domain. The system shows a steady-state error of 14.8 millimetres and a time constant of 0.109 milliseconds at low gain (Kp), showing higher position error but slower response. The time constant rises to 0.293 milliseconds with a middle gain (K_d), but the steady-state error dramatically falls to 3.1 millimetres, indicating a trade-off between response time and positional accuracy. PID control effectively minimises both response time and positional error; with high gain (K_{PID}), the system achieves a fast response with a time constant of 0.054 milliseconds and the lowest steady-state error of 1.5 millimetres. This comparison shows how various gain choices affect the dynamic and steady-state performance of the control system.

4.5. Comparative analysis with different fitness

The nature of the optimisation issue, including its complexity, smoothness of the solution space, gradient information availability, and tolerance for local versus global optima, determines the nonlinear optimisation methods and metaheuristic algorithms. In general, metaheuristics are chosen for exploring complex, uncertain, or highly nonlinear optimisation landscapes. In contrast, nonlinear optimisation techniques are preferred when the problem structure permits accurate computations and deterministic convergence.

4.5.1. Other optimisation techniques

To achieve optimal performance for synchronisation of bilateral teleoperation systems against time delay, the performance of tuned controllers is compared with the gains obtained by several optimisation techniques [23] such as COA, Biogeography-Based Optimization (BBO), Imperialist Competitive Algorithm (ICA), Artificial Bee Colony (ABC), PSO, GA, Ant Colony Optimization with Reinforcement learning (ACOR), Self-adaptive Normalized Differential Evolution (SaNSDE), Adaptive Differential Evolution (JADE), Enhanced Population-Based Incremental Learning (EPSDE), and Cuckoo Search (CS). Optimising synchronisation control parameters for enhanced bilateral teleoperation systems using a PID controller offers several benefits compared to KP and Kd controllers. The PID controller includes an integral component (KI) in addition to the proportional (KP) and derivative (Kd) components, which

https://doi.org/10.1017/S0263574724001565 Published online by Cambridge University Press

enhances the system's ability to eliminate steady-state errors and improve overall accuracy. This results in better tracking stability and performance, particularly in the presence of external forces and time delays. The real-time adaptability of the PID controller to changing conditions leads to smoother and more accurate synchronisation, improving user experience and increasing system reliability. Existing works using only KP and Kd controllers may be highly susceptible to disturbances and variations in system parameters, potentially causing instability or oscillations. Additionally, derivative control can amplify high-frequency noise in the feedback signal, leading to unpredictable and unstable system behaviour. PID controllers are designed to overcome these limitations by integrating the strengths of proportional, integral, and derivative actions. This combination ensures improved performance, stability, and precision in synchronisation control.

Comparison of other techniques over the proposed model. This study compared the proposed model with various metaheuristic algorithms to determine the best performance for synchronising bilateral teleoperation systems. The optimisation algorithms included in the list are CS, JADE, EPSDE, SaNSDE, ICA, ABC, PSO, GA, BBO, COA, and ACOR. These methods are appropriate for various optimisation issues and provide varying convergence speeds while balancing exploration and exploitation. They are renowned for their accuracy over a wide range of difficulties, robustness, fast convergence, and simplicity of implementation. In this study, we used a nonlinear optimisation technique, the SQP-PID controller, and compared it with various metaheuristic algorithms. We could not compare it with other nonlinear optimisation techniques because existing works are not concentrated on employing nonlinear optimisation for synchronisation issues in bilateral telecommunication. Most existing studies have used metaheuristic algorithms for Bilateral Teleoperation Systems. Therefore, we compared the proposed model with these metaheuristic algorithms. In the future, this framework will be extended to include a comparison of nonlinear optimisation techniques. Table II compares the limitations of several optimisation techniques over the proposed model.

The drawbacks of several optimisation techniques include sensitivity to initial conditions and the need for careful parameter tuning. These techniques can also experience delayed convergence in high-dimensional or complex environments, and they often involve significant processing costs when solving large-scale issues. Additionally, there may be a need for parameter modifications, a risk of premature convergence, and system complexity. These techniques may converge slowly in high-dimensional problems and have limited accuracy in complex scenarios. The proposed model aims to overcome these drawbacks, offering better convergence and performance for the synchronisation control of bilateral teleoperation systems.

4.6. Worst fitness

Table III and Fig. 6 showcase the worst fitness scores for various algorithms, illustrating their performance in tackling specific tasks. In fitness evaluation, lower scores indicate better efficiency, making the algorithms with higher values less optimal for the given task. Among the algorithms assessed, GA displays a fitness score of 0.824778, followed closely by PSO at 0.817223, signifying their relatively poor performance. ABC and BBO demonstrate slightly lower scores of 0.797696 and 0.80379, respectively, showing a marginally improved but subpar performance. However, algorithms like ICA and ACOR reveal higher scores of 0.757233 and 0.783745, indicating a less favourable fitness outcome. Further down the line, CS displays a score of 0.750607, while JADE and EPSDE show even higher scores above 1. The algorithms with the least optimal fitness scores include SaNSDE at 0.995551 and COA at 0.732162, highlighting their notably poorer performance than others evaluated in this context. We can determine the algorithm's flexibility to changes in initial conditions and issue cases by comparing the worst fitness values across various algorithms. This data shows that, compared to other well-known optimisation methods, the suggested strategy effectively produces better optimisation results across all three types of controllers.

https://doi.org/10.1017/S0263574724001565 Published online by Cambridge University Press

Table II. *Comparison of limitations of other optimisation techniques over the proposed model.*

Optimisation technique	Convergence speed	Accuracy	Computational complexity	Robustness	Scalability	Limitation
COA	Moderate	High	Medium	High	Medium	It can be sensitive to initial conditions and requires careful parameter tuning.
BBO	Moderate	Medium	High	Medium	Medium	Can struggle with convergence in complex or high-dimensional spaces.
ICA	Slow	Medium	High	Medium	Low	Slower convergence and high computational cost for large-scale problems
ABC	Moderate	Medium	Medium	High	High	It may have slower convergence for specific problems and requires careful parameter setting.
PSO	Fast	High	Low	Medium	High	Can suffer from premature convergence and may need parameter adjustments.
GA	Moderate	High	Medium	High	High	It requires tuning of multiple parameters and can be computationally expensive.
ACOR	Moderate	High	Medium	High	Medium	May require significant computational resources and can be slow for large problems.
SaNSDE	Moderate	High	Medium	High	Medium	Can be complex to implement and may require significant computational resources.
JADE	Moderate	High	Medium	High	Medium	It may need help with very high-dimensional problems and requires careful tuning.
EPSDE	Moderate	High	High	High	Low	High computational complexity and can be slow to converge in some cases.
CS	Fast	Medium	Low	Medium	High	It may need more accuracy for some complex problems and require parameter tuning.

4.7. Mean fitness

A performance spectrum emerges in fitness algorithms, revealing distinct characteristics among various methodologies. When assessing these algorithms based on their mean fitness values, it's apparent that some showcase superior aptitude while others lag. We may ascertain how consistently the algorithm

https://doi.org/10.1017/S0263574724001565 Published online by Cambridge University Press

Table III. *Worst fitness.*

Worst Fitness			
Algorithm	**PID**	**PI**	**PD**
GA	0.824778	4.552874	9.091998
PSO	0.817223	4.729808	9.470771
ABC	0.797696	5.544190	11.148221
BBO	0.80379	5.119710	10.238767
ICA	0.757233	6.452113	12.90127
ACOR	0.783745	5.755437	11.495851
CS	0.750607	7.146932	14.322504
JADE	1.022134	7.409964	14.900532
EPSDE	1.003290	7.334329	14.673035
SaNSDE	0.995551	7.064288	14.068003
COA	0.732162	7.498444	15
Proposed	0.5	0.3	2.5

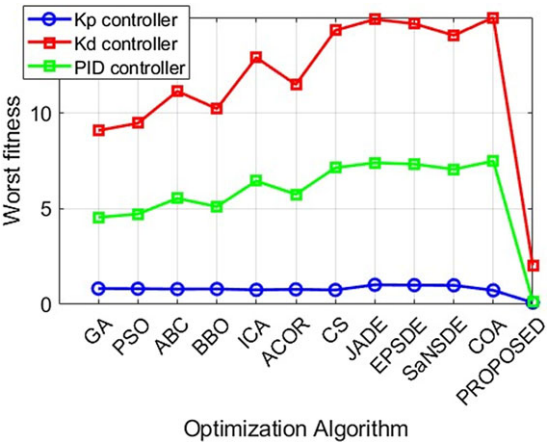


Figure 6. *Comparison graph for worst fitness.*

finds acceptable responses by looking at the mean fitness. A lower mean fitness shows that the algorithm is generally good in various scenarios. Among the contenders, the GA demonstrates a middling performance with a mean fitness of 0.776423, trailing closely to the PSO algorithm at 0.773652. Yet, the ABC algorithm must catch up with a mean fitness of 0.745914, hinting at its struggles in optimisation landscapes.

Similarly, the ICA and the BBO exhibit commendable but not outstanding performances, scoring 0.735631 and 0.762197 in mean fitness, respectively. However, outliers like JADE and EPSDE present intriguing contrasts; while they display higher mean fitness values, 0.985966 and 0.925921, respectively, their performance across other metrics might warrant further investigation. Finally, the CS, Scatter Search with Local Descent, and different algorithms reveal consistent patterns, hovering around the 0.74 – 0.76 range for mean fitness, showcasing stability but potentially lacking in exceptional performance. Notably, the COA algorithm (COA) presents a mean fitness of 0.732139, hinting at its struggles to find optimal solutions within the fitness landscape. This spectrum of fitness metrics offers insights into the varied performances of these algorithms, inviting deeper scrutiny into their methodologies and potential areas for improvement. This data shows that, compared to other well-known optimisation techniques, the suggested strategy is remarkably effective at consistently producing better optimisation outcomes

https://doi.org/10.1017/S0263574724001565 Published online by Cambridge University Press

Table IV. *Mean fitness.*

Mean Fitness			
Algorithm	**PID**	**PI**	**PD**
GA	0.776423	6.099495	12.202223
PSO	0.773652	6.217929	12.435981
ABC	0.745914	7.024489	14.057926
BBO	0.762197	6.376495	12.751097
ICA	0.735631	7.355015	14.710518
ACOR	0.745794	7.500189	14.810435
CS	0.743635	7.396619	14.802649
JADE	0.985966	7.484704	14.956088
EPSDE	0.925921	7.473836	14.894829
SaNSDE	0.959299	7.365747	14.744262
COA	0.732139	7.500205	15
Proposed	0.1	0.2	0.15

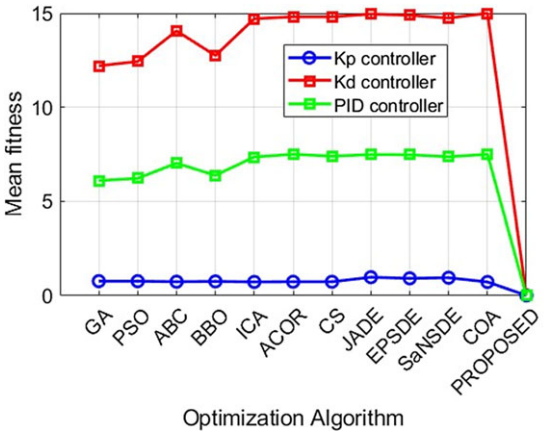


Figure 7. *Comparison graph for mean fitness.*

for all controllers. Table IV and Fig. 7 present the algorithms' mean fitness ratings to demonstrate how well different algorithms perform when faced with particular tasks.

4.8. Best fitness

Table V and Fig. 8 showcase the performance metrics of the best fitness algorithms, ranging from the worst to the best fitness scores across different parameters. In the realm of PID algorithms, the least effective in fitness improvement is the ABC algorithm with a score of 0.732150, closely followed by ICA and COA, sharing the same fitness score of 0.732135. Moving along the spectrum towards more effective fitness enhancement, algorithms like PSO and BBO demonstrate slightly higher scores of 0.742116 and 0.738460, respectively, depicting moderate performance. The ACOR and CS algorithms display a comparable fitness level of 0.742116 and 0.742116, respectively, a notch higher than the previous ones. However, the most impressive enhancement in fitness is observed in algorithms like JADE with a score of 0.908048, EPSDE at 0.763318, and SaNSDE scoring 0.904672, showcasing substantial improvements. These algorithms demonstrate significantly better fitness in their respective methodologies, positioning them at the apex of the fitness evaluation among the listed algorithms. The best fitness value indicates the algorithm's most optimal solution. It displays the algorithm's optimal result and its peak performance.

https://doi.org/10.1017/S0263574724001565 Published online by Cambridge University Press

Table V. *Best fitness.*

Best Fitness			
Algorithm	**PID**	**PI**	**PD**
GA	0.751330	7.062972	14.115096
PSO	0.742116	7.130208	14.253315
ABC	0.732150	7.498933	15
BBO	0.738460	7.205131	14.412602
ICA	0.732135	7.500426	15
ACOR	0.742116	7.500189	14.99999
CS	0.742116	7.500130	15
JADE	0.908048	6.99580	14.015897
EPSDE	0.763318	6.954063	14.979631
SaNSDE	0.904672	7.464771	14.9405234
COA	0.732135	7.500397	15
Proposed	0.1	3.5	2.5

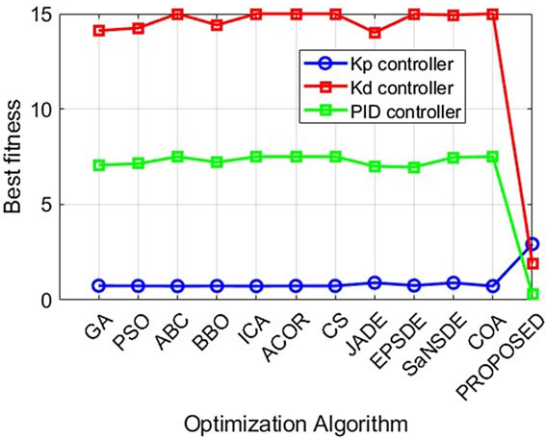


Figure 8. *Comparison graph for best fitness.*

The algorithms can be evaluated against one another by comparing their best fitness value and finding the best outcomes.

The results highlight the effectiveness of the SQP-PID algorithm's control structure, which achieves superior convergence speed in position tracking despite starting from a nonzero offset. This implies that even with the initial discrepancy between the master and slave joint angles (0.4 units offset), the control approach enables the slave to converge accurately to the joint angle of the master. Time delays can disrupt synchronisation between the master and slave, causing inaccuracies or instability. However, the control method mitigates this issue, enabling effective tracking despite the delay. It emphasises the robustness of this proposed control structure in dealing with two critical factors: time delay in communication channels and parameter uncertainty with accurate outcomes in handling delays inherent in communication channels. Despite the delay in receiving information or commands from the master, the slave converges accurately to the desired joint angle. This implies that the control approach incorporates mechanisms to compensate for or predict the effects of these delays. Also, the control structure exhibits robustness against such uncertainties, indicating that it can adapt or adjust its strategies to accommodate variations in system parameters. The abovementioned control structure achieves optimal performance,

https://doi.org/10.1017/S0263574724001565 Published online by Cambridge University Press

but the control structure keeps the system stable even in the face of unclear or variable system characteristics. This indicates that the control approach is designed to handle parameter variations without compromising its stability or performance. In control systems, like bilateral teleoperation, the application of SQP rationalises effective parameter optimisation under nonlinear constraints. Because of SQP's capacity to manage intricate dynamics and stringent operating constraints, control performance is robustly maintained, improving system responsiveness and stability. This robustness and adaptability make it a promising approach for ensuring accurate position tracking and stability in such challenging scenarios, as seen in the figure. We may examine the algorithm's convergence behaviour by tracking the patterns in the worst, mean, and best fitness values over iterations. Convergence towards ideal solutions is indicated by a decreasing difference between the worst and best fitness values over time. This examination aids in comprehending how fast and steadily the algorithm converges to superior solutions.

5. Conclusion

In conclusion, this study addresses a critical challenge in bilateral teleoperation systems – synchronisation discrepancies due to communication delays. Recognising the limitations of conventional control methods, the research introduces a groundbreaking solution employing SQP optimisation for PID controllers. By comprehensively modelling the dynamics and intricacies of communication, this work pioneers an SQP-PID controller that effectively mitigates synchronisation errors. Unlike traditional PD controllers, this novel approach compensates for delays, ensuring precise control without steady-state deviations. The standout feature lies in its capacity to handle steady-state errors efficiently while swiftly responding to maintain stability. This controller uses the SQP optimisation algorithm to tune parameters, minimising synchronisation discrepancies intelligently. Since SQP can be a computationally intensive technique, it may not be appropriate for systems with low processing capacity or requiring rapid response times. The additional computational resources and possible costs of implementing sophisticated optimisation techniques like SQP may be prohibitive for specific applications or industries. The simplicity, performance, and robustness of the SQP-PID controller offer a promising avenue for significantly enhancing the accuracy and stability of bilateral teleoperation systems, exhibiting remarkable results with a best fitness value of 0.98% across diverse operating conditions. This innovation marks a substantial leap towards achieving excellent reliability and precision in real-time teleoperation scenarios. The study will include multi-agent teleoperation systems, which need more complex synchronisation and control schemes due to the interaction of numerous master and slave units.

Author contribution. **First author:** Naveen Kumar
Writing original draft, methodology, study conception and design, reviewing and editing
Second author (Corresponding author): Niharika Thakur
Conceptualisation, data collection, reviewing and editing
Third author: Yogita Gupta
Analysis and interpretation of results, reviewing and editing

Financial support. No fund was received for this work.

Competing interests. On behalf of all authors, the corresponding author states that they have no competing interest.

Ethics approval and consent to participate. This article does not contain any studies with human participants or animals performed by any of the authors.

Consent for publication. All contributors agreed and given consent to publication.

Availability of data and material. Data that has been used is confidential.

https://doi.org/10.1017/S0263574724001565 Published online by Cambridge University Press

References

[1] N. Kumar, N. Thakur and Y. Gupta, "Time delay compensated disturbance observer-based sliding mode slave controller and neural network model for bilateral teleoperation system," *Intell Serv Robot* **17**, 1–13 (2024).

[2] R. N. Elek and T. Haidegger, "Robot-assisted minimally invasive surgical skill assessment—Manual and automated platforms," *Acta Polytech Hung* **16**(8), 141–169 (2019).

[3] C. B. Beaman, N. Kaneko, P. M. Meyers and S. Tateshima, "A review of robotic interventional neuroradiology," *Am J Neuroradiol* **42**(5), 808–814 (2021).

[4] N. Hameedha and A. Mohideen, Network Delay Mitigated Remote Robot Control with Force Feedback for Improved QoS (2022).

[5] F. Wang, Z. Qian, Y. Lin and W. Zhang, "Design and rapid construction of a cost-effective virtual haptic device," *IEEE/ASME Trans Mechatr* **26**(1), 66–77 (2020).

[6] G. Lunghi, R. Marin, M. Di Castro, A. Masi and P. J. Sanz, "Multimodal human-robot interface for accessible remote robotic interventions in hazardous environments," *IEEE Access* **7**, 127290–127319 (2019).

[7] Y. Yan, Y. Liu, J. Fang, Y. Lu and X. Jiang, "Application status and development trends for intelligent perception of distribution network," *High Volt* **6**(6), 938–954 (2021).

[8] J.O. Bolarinwa, Enhancing Tele-Operation-Investigating the Effect of Sensory Feedback On Performance (Faculty of Engineering and Technology, University of the West of England, Bristol, 2022). Doctoral dissertation

[9] N. Kumar, N. Thakur and Y. Khanna, "Time delay Independent of Bilateral Tele-Robotic System using Wave Variable Approach," **In:** *2022 8th International Conference on Signal Processing and Communication (ICSC)*, (2022) pp. 669–674.

[10] N. Thakur, Y. K. Awasthi, M. Hooda and A. S. Siddiqui, "Adaptive whale optimization for intelligent multi-constraints power quality improvement under deregulated environment," *J Eng Des Technol* **17**(3), 490–514 (2019).

[11] D. Mariano-Hernández, L. Hernández-Callejo, A. Zorita-Lamadrid, O. Duque-Pérez and F. S. García, "A review of strategies for building energy management system: Model predictive control, demand side management, optimization, and fault detect & diagnosis," *J Build Eng* **33**, 101692 (2021).

[12] H. J. Kaleybar, M. Davoodi, M. Brenna and D. Zaninelli, "Applications of genetic algorithm and its variants in rail vehicle systems: A bibliometric analysis and comprehensive review," *IEEE Access* **11**, 68972–68993 (2023).

[13] M. Nasr, M. M. Islam, S. Shehata, F. Karray and Y. Quintana, "Smart healthcare in the age of AI: Recent advances, challenges, and future prospects," *IEEE Access* **9**, 145248–145270 (2021).

[14] S. Alahakoon, R. B. Roy and S. J. Arachchillage, "Optimizing load frequency control in standalone marine microgrids using meta-heuristic techniques," *Energies* **16**(13), 4846 (2023).

[15] H. Lyu, D. Kong, G. Pang, B. Wang, Z. Yu, Z. Pang and G. Yang, "GuLiM: A hybrid motion mapping technique for teleoperation of medical assistive robot in combating the COVID-19 pandemic," *IEEE Trans Med Robot Bio* **4**(1), 106–117 (2022).

[16] Y. Su, L. Lloyd, X. Chen and J. G. Chase, "Latency mitigation using applied HMMs for mixed reality-enhanced intuitive teleoperation in intelligent robotic welding," *Int J Adv Manuf Technol* **126**(5-6), 2233–2248 (2023).

[17] H. Shokri-Ghaleh, A. Alfi, S. Ebadollahi, A. M. Shahri and S. Ranjbaran, "Unequal limit cuckoo optimization algorithm applied for optimal design of nonlinear field calibration problem of a triaxial accelerometer," *Measurement* **164**, 107963 (2020).

[18] W. U. Rehman, X. Wang, Z. Hameed and M. Y. Gul, "Motion synchronization control for a large civil aircraft's hybrid actuation system using fuzzy logic-based control, techniques," *Mathematics* **11**(7), 1576 (2023).

[19] L. Mohammadi and A. Alfi, "Guaranteed cost control in delayed teleoperation systems under actuator saturation," *Iran J Sci Technol Trans Electr Eng* **43**(4), 827–835 (2019).

[20] Y. Ishiguro, T. Makabe, Y. Nagamatsu, Y. Kojio, K. Kojima, F. Sugai and M. Inaba, "Bilateral humanoid teleoperation system using whole-body exoskeleton cockpit TABLIS," *IEEE Robot Autom Lett* **5**(4), 6419–6426 (2020).

[21] F. Naseer, M. N. Khan and A. Altalbe, "Intelligent time delay control of telepresence robots using novel deep reinforcement learning algorithm to interact with patients," *Appl Sci* **13**(4), 2462 (2023).

[22] P. R. Ouyang, T. Dam, J. Huang and W. J. Zhang, "Contour tracking control in position domain," *Mechatronics* **22**(7), 934–944 (2012).

[23] H. Shokri-Ghaleh and A. Alfi, "A comparison between optimization algorithms applied to synchronization of bilateral teleoperation systems against time delay and modeling uncertainties," *Appl Soft Comput* **24**, 447–456 (2014).

Cite this article: N. Kumar, N. Thakur and Y. Gupta (2024). "Optimisation of synchronisation control parameters for enhanced bilateral teleoperation system", Robotica **42**, 3639–3656. https://doi.org/10.1017/S0263574724001565

https://doi.org/10.1017/S0263574724001565 Published online by Cambridge University Press